# Probing the Incompressibility of Nuclear Matter at Ultrahigh Density through the Prompt Collapse of Asymmetric Neutron Star Binaries

Albino Perego,[1,2,*] Domenico Logoteta,[3,4] David Radice,[5,6,7] Sebastiano Bernuzzi,[8] Rahul Kashyap,[5,6] Abhishek Das,[5,6] Surendra Padamata,[5,6] and Aviral Prakash[5,6]

[1]*Dipartimento di Fisica, Università di Trento, Via Sommarive 14, 38123 Trento, Italy*
[2]*INFN-TIFPA, Trento Institute for Fundamental Physics and Applications, Via Sommarive 14, I-38123 Trento, Italy*
[3]*Dipartimento di Fisica, Università di Pisa, Largo B. Pontecorvo 3, I-56127 Pisa, Italy*
[4]*INFN, Sezione di Pisa, Largo B. Pontecorvo 3, I-56127 Pisa, Italy*
[5]*Institute for Gravitation and the Cosmos, Pennsylvania State University, University Park, Pennsylvania 16802, USA*
[6]*Department of Physics, Pennsylvania State University, University Park, Pennsylvania 16802, USA*
[7]*Department of Astronomy and Astrophysics, Pennsylvania State University, University Park, Pennsylvania 16802, USA*
[8]*Theoretisch-Physikalisches Institut, Friedrich-Schiller Universität Jena, 07743 Jena, Germany*

(Received 10 December 2021; revised 16 March 2022; accepted 6 June 2022; published 13 July 2022)

Using 250 neutron star merger simulations with microphysics, we explore for the first time the role of nuclear incompressibility in the prompt collapse threshold for binaries with different mass ratios. We demonstrate that observations of prompt collapse thresholds, either from binaries with two different mass ratios or with one mass ratio but combined with the knowledge of the maximum neutron star mass or compactness, will constrain the incompressibility at the maximum neutron star density $K_{\max}$ to within tens of percent. This otherwise inaccessible measure of $K_{\max}$ can potentially reveal the presence of hyperons or quarks inside neutron stars.

DOI: 10.1103/PhysRevLett.129.032701

*Introduction.*—The equation of state (EOS) of neutron star (NS) matter is one of the most fundamental, yet elusive, relations in physics [1,2]. It lays at the interface between several disciplines, including nuclear physics, high-energy astrophysics, heavy-ion collisions, multimessenger astronomy, and gravitational wave (GW) physics. Our knowledge of NS matter properties is still partial, mostly due to the difficulties in studying strongly interacting bulk matter in the low-energy limit typical of nuclear interactions [3]. Even the appropriate degrees of freedom are uncertain: while nucleons are the relevant species around the nuclear saturation density, $n_0 = 0.16\ \mathrm{fm}^{-3}$, it is still unclear if hyperons [4,5] or a phase transition to quark matter [6–8] can appear at densities $n \gtrsim 2n_0$ in NS interiors.

NS EOS models are experimentally constrained by the masses of ordinary nuclei, as well as by the energy per baryon and its derivatives with respect to baryon density $n_b$ around $n_0$ and close to isospin symmetry, i.e., for symmetry parameter $\delta \equiv (n_n - n_p)/n_b \approx 0$, with $n_{n,p}$ being the density of neutrons and protons. If $P$ is the matter pressure, the nuclear incompressibility of cold nuclear matter at fixed composition is defined as

$$K(n_b, \delta) \equiv 9 \left. \frac{\partial P}{\partial n_b} \right|_{T=0, \delta=\mathrm{const}}. \quad (1)$$

It describes the response of matter to compression and its value can be currently measured only for symmetric matter at saturation density $K_{\mathrm{sat}}$, although with some controversy [9–13]. While isoscalar giant monopole resonance experiments for closed-shell nuclei provided $K_{\mathrm{sat}} = (240 \pm 20)$ MeV, studies based on open-shell nuclei reported quite different values in the range 250–315 MeV [12] or even values around 200 MeV [13]. Nevertheless, $K_{\mathrm{sat}}$ is unconstrained at densities and compositions relevant for NSs (far from $n \approx n_0$ and $\delta \approx 0$). In particular, according to the solutions of the Tolman-Oppenheimer-Volkoff (TOV) equation, the NS central density increases monotonically with the NS mass and at the stability limit, corresponding to mass and radius ($M_{\max}^{\mathrm{TOV}}$, $R_{\max}^{\mathrm{TOV}}$), can reach $n_{\max}^{\mathrm{TOV}} \sim 4$–$7n_0$, depending on the EOS. Moreover, for $n_b \gtrsim n_0$, $\beta$-equilibrated matter is very neutron rich, $\delta_{\mathrm{eq}} \sim 1$.

In addition to nuclear constraints, astrophysical NS properties provide useful insights on the EOS. Constraints derived from the observation of massive, isolated NSs [14–20], from GW signals [21,22], and multimessenger observations of binary neutron star (BNS) mergers [23–28], or by their combination [29,30], are very informative about the high-density regime. A key phenomenon in this respect is the prompt collapse (PC) to black hole (BH) of the merger remnant, since this behavior can influence both the GW and electromagnetic (EM) signals produced by BNS mergers [31–36]. The PC behavior of equal mass BNSs was extensively explored in Refs. [37–43]. It was shown, for example, that the

 

threshold mass for PC $M_{\rm th}$, normalized to $M_{\rm max}^{\rm TOV}$, linearly correlates with the maximum compactness, defined as $\mathcal{C}_{\rm max}^{\rm TOV} \equiv GM_{\rm max}^{\rm TOV}/(R_{\rm max}^{\rm TOV}c^2)$, where $c$ and $G$ are the speed of light and the gravitational constant, respectively, as well as with other NS equilibrium properties. More recently, also the study of asymmetric BNS mergers has received attention [42,44–46]. Bauswein *et al.* [42,44] concluded that PC in asymmetric BNSs usually occurs for masses equal or smaller than in the equal mass case, with the possible exception of modest asymmetries and very soft equations of state. The total mass reduction is stronger for more extreme mass ratios and it has a nontrivial dependence on the NS EOS. Tootle *et al.* [45] suggested instead a quasiuniversal relation. In all these Letter, several fitting formulas to numerical results were provided.

In this Letter, we show that $K_{\rm max}$, the incompressibility of nuclear, $\beta$-equilibrated matter at $n_{\rm max}^{\rm TOV}$, determines the behavior of BNS mergers close to PC and, in particular, their dependence on the mass ratio. Our results stem from the largest set of numerical relativity simulations of irrotational, asymmetric binaries with finite-temperature, composition-dependent microphysical equations of state to date. We demonstrate that the detection of $M_{\rm th}$ at two different mass ratios can provide a direct measurement of $K_{\rm max}$ in a regime otherwise inaccessible. Additionally, we suggest that its value can yield information about the relevant thermodynamics degrees of freedom close to $n_{\rm max}^{\rm TOV}$.

*Methods and models.*—We simulate 250 irrotational BNS mergers with different gravitational masses $M \equiv M_1 + M_2 \in [2.786\ M_\odot, 3.3\ M_\odot]$ and mass ratios $q \equiv M_1/M_2 \in \{0.6, 0.65, 0.7, 0.75, 0.85, 1\}$. We perform a series of simulations at fixed $q$ while changing $M$ to explore the onset of the PC behavior and determine $M_{\rm th}(q)$. For the definition of $M_{\rm th}(q)$ and its numerical error $\delta M_{\rm th}(q)$, we follow Refs. [42,43,47], monitoring the minimum of the lapse function throughout the computational domain. Simulations are performed with the same codes and setup as in Ref. [43]; $q = 1$ data are from Ref. [43], while $q \neq 1$ data are presented here for the first time. See the Supplemental Material [48] for more details, which includes also Refs. [49–91].

To span present uncertainties, we consider six finite-temperature, composition-dependent NS equations of state. Four are purely nucleonic and widely used: BL [92,93], SFHo [94], HS(DD2) (hereafter DD2) [95,96], and LS220 [97]. Additionally, we consider an EOS including hyperons, HS(BHB$\Lambda\phi$) (hereafter, BHB) [98], and one including a phase transition to quark matter, DD2qG, also presented in Ref. [43]. In both cases, the nucleonic baseline is DD2. In Fig. 1, we present the nuclear incompressibility of neutrinoless, $\beta$-equilibrated, cold NS matter $K_{\rm eq}$, defined as in Eq. (1) but for $\delta = \delta_{\rm eq}$, for the six different equations of state above as a function of $n_b$. For each EOS we highlight $K_{\rm max} \equiv K(n_{\rm max}^{\rm TOV})$. It is striking that the properties in the low-density regime ($n_b < 2n_0$) do not necessarily correlate with those at $n_b \sim n_{\rm max}^{\rm TOV}$. Moreover, the BL, SFHo, and LS220 equations of state, despite being softer than the DD2 EOS, reach larger $n_{\rm max}^{\rm TOV}$ and provide similar, if not larger, $K_{\rm max}$.

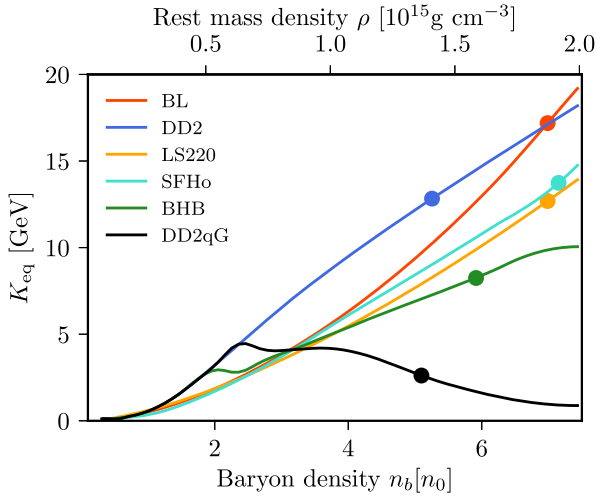


FIG. 1. Nuclear incompressibility $K_{\rm eq}$ of cold $\beta$-equilibrated nuclear matter as a function of baryon density for the EOS employed in this Letter. Solid markers correspond to $K_{\rm max}$, i.e., $K_{\rm eq}$ at the central density of the heaviest irrotational NS.

*Results.*—Our simulations robustly indicate that PC occurs as the maximum of the rest mass density throughout the computational domain, $n_{\rm max}$ approaches $n_{\rm max}^{\rm TOV}$ at merger. With the exception of the DD2qG EOS, for which $n_{\rm max} \sim 0.8$–$1.2 n_{\rm max}^{\rm TOV}$, for the heaviest non-PC BNS we observe $n_{\rm max} \sim 0.75$–$0.95 n_{\rm max}^{\rm TOV}$ at the first remnant bounce, with larger values usually associated with $q \sim 1$. Two opposite effects influence the evolution of $n_{\rm max}$ with respect to $q$. On the one hand, for a given $M$, binaries with smaller $q$'s have smaller orbital angular momentum and the NS cores are more prone to fuse (and thus to increase $n_{\rm max}$ toward $n_{\rm max}^{\rm TOV}$) due to the smaller rotational support [42,44]. On the other hand, the nuclear incompressibility usually increases as $n_{\rm max}$ grows, providing a larger nuclear repulsion that contrasts its further increase. Since PC is observed for $n_{\rm max} \sim n_{\rm max}^{\rm TOV}$, it is understandable that $K_{\rm max}$ is the incompressibility value relevant for the PC behavior.

To analyze the dependence of PC on $K_{\rm max}$, in Fig. 2 we first consider $f(q) \equiv M_{\rm th}(q)/M_{\rm th}(q=1)$ for all equations of state, where (to be conservative) the error bars have been obtained by propagating the errors both on $M_{\rm th}(q)$ and $M_{\rm th}(q=1)$. Values of $M_{\rm th}$ and $\delta M_{\rm th}$ are reported in the Supplemental Material [48]. We first observe that our results do not have a universal behavior for the different equations of state. Second, we notice that a variation of almost a factor of 1.7 in $q$ has a small effect on $M_{\rm th}(q)$, with the corresponding variation in $f(q)$ ranging between 3% and 8%, larger for equations of state with a smaller $K_{\rm max}$. This is broadly compatible to what was observed in [42,44–46] and should

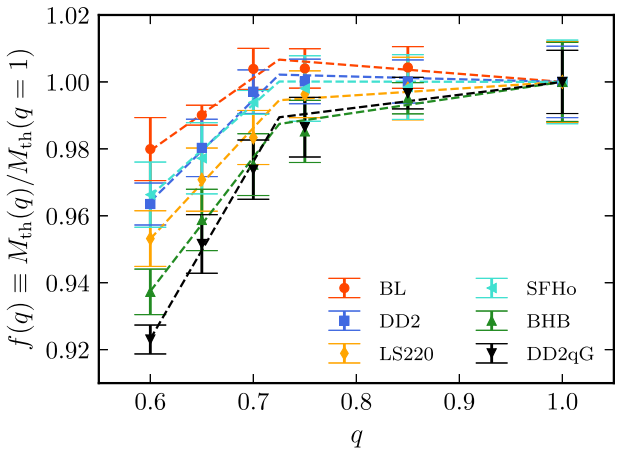


FIG. 2. Threshold PC masses normalized to the $q = 1$ case as a function of $q$ for all the equations of state used in this Letter. Dashed lines correspond to Eq. (2) fit.

be compared with the larger ($\lesssim$20%) variation in $M_{\rm max}^{\rm TOV}$ or $M_{\rm th}(q=1)/M_{\rm max}^{\rm TOV}$ reported in Refs. [34,38,40–43,47].

Focusing on the behavior of $f(q)$ for $0.7 \lesssim q \leq 1$ we observe that, depending on the EOS, $f(q)$ can decrease, stay approximately constant, or even increase as $q$ decreases (see also Refs. [44,46,99]). We interpret this as the result of the interplay between the binary orbital angular momentum and the incompressibility of nuclear matter, in light of the merger dynamics. For BNSs with $q \lesssim 1$ and $M \approx M_{\rm th}$, the central density inside the more massive NS ranges is 0.40–0.49 $n_{\rm max}$ (depending on the EOS) and the merger is driven by the fusion of two comparable NS cores. If $K_{\rm eq}$ increases steeply enough with $n_{\rm max}$, nuclear repulsion contrasts efficiently gravity-driven compression. The net result is that for equations of state with a relatively large $K_{\rm max}$ (as BL, SFHo, and DD2), $M_{\rm th}(q \lesssim 1)$ can stay rather constant or even increase as $q$ decreases. On the other hand, if $K_{\rm eq}$ does not increase significantly with $n_b$ and $K_{\rm max}$ is relatively low (as for DD2qG and BHB), nuclear repulsion is not enough to counterbalance the lack of rotational support and PC occurs for $M_{\rm th}(q \lesssim 1) < M_{\rm th}(q = 1)$.

Moving to $0.6 \lesssim q \lesssim 0.7$, we notice a clear change of behavior: $f(q)$ decreases as $q$ decreases for all equations of state. But, once again, the variation depends sensitively on $K_{\rm max}$: equations of state characterized by a smaller $K_{\rm max}$ result not only in smaller $f(q)$, but also in larger relative variations with respect to $f(q \approx 0.7)$. We explain this transition in terms of the different merger dynamics. For BNSs at the PC threshold and with $q \lesssim 0.7$, the central density inside the more massive NS increases to 0.5–0.57 $n_{\rm max}^{\rm TOV}$, while the secondary NS is more significantly deformed and tidally disrupted during the last orbits. As $q$ decreases, the denser core of the more massive NS is compressed by more massive streams of accreting matter [33,36,42,100,101]. The nuclear incompressibility still opposes compression, but less efficiently than in the $0.7 \lesssim q \leq 1$ regime. $K_{\rm max}$ still provides a measure of the NS matter resistance to compression in the relevant density interval and different equations of state result in different relative variations.

Our data qualitatively agree with those from independent simulations recently reported in Refs. [41,45,46]. However, quantitative differences comparable to the overall variation observed in our results are found. This is possibly due to different definitions of PC threshold, gravity treatment, or numerical resolutions. A comparison with the some of the available fits is reported in the Supplemental Material [48]. Moreover, our extended set of equations of state indicates a subleading but significant and systematic EOS dependence emerging for asymmetric binaries, in contrast to a quasiuniversal behavior [45].

Figure 2 suggests the existence of two different regimes, separated by $0.7 \lesssim \tilde{q} \lesssim 0.75$, which is largely independent from the EOS. In each of the two regimes, $f(q)$ is well described by a linear relation. Thus, for each EOS we fit our data by considering

$$f(q) = \alpha(q)q + \beta(q) = \begin{cases} \alpha_l q + \beta_l & \text{if } q < \tilde{q}, \\ \alpha_h q + \beta_h & \text{if } q \geq \tilde{q}. \end{cases} \quad (2)$$

We fix $\beta_{l,h}$ in Eq. (2) by imposing the continuity of $f(q)$ at $q = \tilde{q}$ and $f(q = 1) = 1$. Moreover, we assume $\tilde{q} = 0.725$ by closely inspecting Fig. 2. Least-square fits (dashed lines) are performed on the two parameters $\alpha_{l,h}$, corresponding to the slopes of the two linear regimes. The residuals relative to the errors are always smaller than 0.5 and without clear systematic trends both with respect to the EOS and $q$.

Our simulations reveal a correlation between $\alpha_{l,h}$ and $K_{\rm max}$, supporting the interpretation that the latter is one of the key properties that control the PC. In Fig. 3, we represent $\alpha_{l,h}$ with their uncertainties as a function of $K_{\rm max}$ for each EOS. Given the reduced number of equations

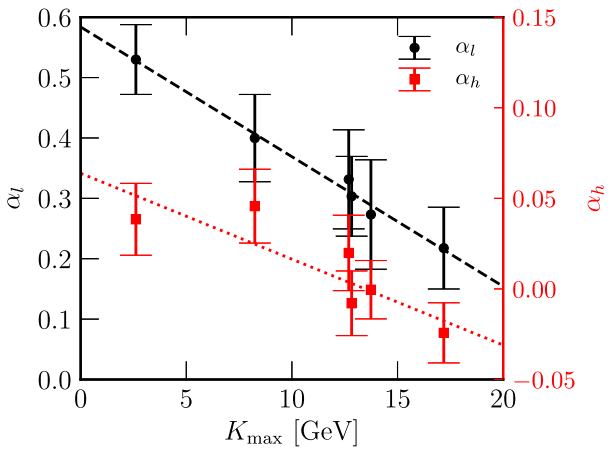


FIG. 3. Slopes of the fitting coefficients $\alpha_{l,h}$ for data in Fig. 2 as a function of $K_{\rm max}$. Both slopes show a trend with $K_{\rm max}$ that we fitted with a linear function (dashed lines).

of state and the relatively large uncertainties, we fit $\alpha_{l,h}$ with a first-order polynomial in $K_{\rm max}$ (dashed lines in Fig. 3),

$$\alpha_l = -(22 \pm 1)\ \mathrm{TeV}^{-1} K_{\rm max} + (0.58 \pm 0.01),$$
$$\alpha_h = -(4.7 \pm 1.0)\ \mathrm{TeV}^{-1} K_{\rm max} + (0.064 \pm 0.017). \quad (3)$$

The slopes of the linear behaviors observed in Fig. 2 usually decrease as the incompressibility increases. This confirms that equations of state with a large incompressibility provide a possible increase in $M_{\rm th}$ for $\tilde{q} < q \leq 1$ and a less steep decrease for $q < \tilde{q}$.

*Discussion.*—Our results suggest that the determination of $M_{\rm th}$ at two different $q$'s, $q_{1,2}$, allows one to determine $K_{\rm max}$ by solving

$$\frac{M_{\rm th}(q_1)}{M_{\rm th}(q_2)} = \frac{\alpha(K_{\rm max}, q_1) q_1 + \beta(\alpha)}{\alpha(K_{\rm max}, q_2) q_2 + \beta(\alpha)}, \quad (4)$$

where $\alpha$ and $\beta$ are defined consistently with Eqs. (2) and (3). To test this, we repeat the previous fits excluding results from the SFHo equations of state. The new fitted coefficients $\alpha'_{l,h}$ are compatible to within uncertainties with $\alpha_{l,h}$ in Eq. (3). We deduce $K_{\rm max}$ for SFHo using these new fits and the $M_{\rm th}(q)$ SFHo results at two different $q$'s. In particular, we randomly sample the intervals $[M_{\rm th}(q) \pm \delta M_{\rm th}(q)/2]$ 1000 times to set simulated values for the threshold masses $\tilde{M}_{\rm th}(q_{1,2})$ and to compute $\tilde{K}_{\rm max}$ by solving Eq. (4). We finally extract the average relative discrepancy between the computed and actual values. For example, using $M_{\rm th}(q = 0.65)$ and $M_{\rm th}(q = 0.85)$, we recover $K_{\rm max}$ to within 2% of its actual value. The uncertainty increases when considering $M_{\rm th}(q = 0.7)$ and $M_{\rm th}(q = 0.85)$. In this case, $K_{\rm max}$ is recovered to within 15%. Our method does not necessarily require the knowledge of $M_{\rm th}(q)$ at two $q \neq 1$. For example, using $M_{\rm th}(q = 0.7)$ and $M_{\rm th}(q = 1)$ we recover $K_{\rm max}$ within 3.5%. The above discrepancies on $K_{\rm max}$ are compatible with the uncertainties implied by Fig. 3.

To further challenge our method, we consider the independent results for $M_{\rm th}(q)$ from Ref. [45] obtained for irrotational NSs and for the TNTYST EOS [102], an EOS not included in our sample and for which $K_{\rm max} > 20$ GeV [We notice, however, that the TNTYST EOS becomes acausal close to $n^{\rm TOV}_{\rm max}$].We consider the $\alpha_{l,h}$ fits, Eq. (3), and we solve Eqs. (4) and (5) using $M_{\rm th}(q = 0.7)$ and $M_{\rm th}(q = 0.9)$. Despite possible systematical differences related to the different way to determine $M_{\rm th}$, we recover the expected value of $K_{\rm max}$ to within 25% (∼6 GeV) of its actual value.

Prompted by these results, we investigate a direct correlation between $\mathcal{C}^{\rm TOV}_{\rm max}$ and $K_{\rm max}$ and we find that the values of $K_{\rm max}$ can provide information on the relevant degrees of freedom in ultradense matter. In Fig. 4, we present $K_{\rm max}$ as a function of $\mathcal{C}^{\rm TOV}_{\rm max}$ for a large set of equations of state. In particular, we selected equations

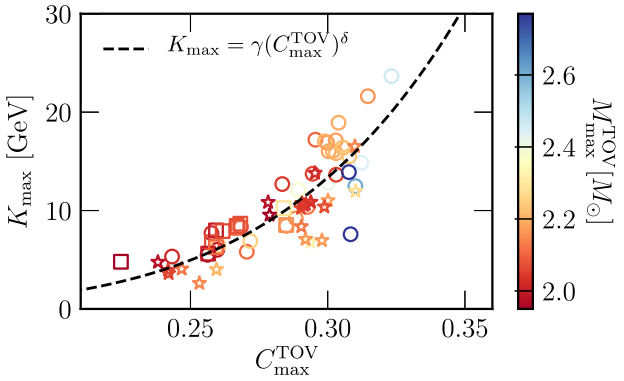


FIG. 4. $K_{\rm max}$ as a function of the compactness of the heaviest NS for a large sample of equations of state. Circles correspond to nucleonic equations of state, while squares and stars correspond to equations of state containing hyperons or undergoing a phase transition to quarks, respectively.

of state that stay causal up to $n^{\rm TOV}_{\rm max}$ and for which $M^{\rm TOV}_{\rm max} > 1.97\ M_\odot$. More detailed information can be found in the Supplemental Material [48]. Different symbols refer to different particle contents, while colors refer to $M^{\rm TOV}_{\rm max}$. We suggest that large $K_{\rm max}(\gtrsim 15$ GeV) are more easily associated with purely nucleonic equations of state, while equations of state containing hyperons or showing a phase transition to quarks are characterized by small $K_{\rm max}(\lesssim 15$ GeV). A tighter threshold at 12 GeV can be observed if only two equations of state containing just $u$ and $d$ quarks, out a sample of 34 equations of state containing quarks or hyperons, were removed. Moreover, $K_{\rm max}$ can be fitted in good approximation with a power law, $K_{\rm max} = \gamma(\mathcal{C}^{\rm TOV}_{\rm max})^{\delta}$. Standard least-squared methods provide $\gamma = (9.2 \pm 5.4)$ TeV and $\delta = 5.67 \pm 0.50$. Despite not being trivial, such a relation is not surprising, since both $M^{\rm TOV}_{\rm max}$ and $R^{\rm TOV}_{\rm max}$ depend on the equilibrium response of the heaviest NS to radial perturbations for $n_b \sim n^{\rm TOV}_{\rm max}$, and thus on $K_{\rm max}$. Moreover, it provides a possible connection between our findings and previous, different fits for $M_{\rm th}$ expressed in terms of $M^{\rm TOV}_{\rm max}$ and $\mathcal{C}^{\rm TOV}_{\rm max}$, both for symmetric and asymmetric mergers [39,40,42–44,46]. For example, we have repeated our analysis in terms of $\mathcal{C}^{\rm TOV}_{\rm max}$ rather than $K_{\rm max}$, finding comparable results, as reported in the Supplemental Material [48]. Even if this relation directly connects $K_{\rm max}$ to $\mathcal{C}^{\rm TOV}_{\rm max}$, we stress that $K_{\rm max}$ provides a cleaner and more intuitive physical interpretation of the PC behavior for $q \neq 1$.

This $K_{\rm max}(\mathcal{C}^{\rm TOV}_{\rm max})$ relation, combined with the linear relation $M_{\rm th}(q = 1)/M^{\rm TOV}_{\rm max} = a\mathcal{C}^{\rm TOV}_{\rm max} + b$ first proposed in Ref. [39] but with coefficients from Ref. [43], suggests that $M^{\rm TOV}_{\rm max}$ can be also related to $K_{\rm max}$ and $M_{\rm th}(q = 1)$,

$$M^{\rm TOV}_{\rm max} = \frac{M_{\rm th}(q = 1)}{a(K_{\rm max}/\gamma)^{1/\delta} + b}. \quad (5)$$

Equations (2) and (5) together suggest that $K_{\rm max}$ can be estimated by the knowledge of only one $M_{\rm th}(q)$, if $M_{\rm max}^{\rm TOV}$ is known,

$$\frac{M_{\rm th}(q)}{M_{\rm max}^{\rm TOV}[a(K_{\rm max}/\gamma)^{1/\delta}+b]} = \alpha(K_{\rm max},q)q+\beta(\alpha). \quad (6)$$

For example, using the $\alpha'_{l,h}$ fits while employing $M_{\rm max}^{\rm TOV}$ and $M_{\rm th}(q=0.85)$ SFHo results as input data, we recover $K_{\rm max}$ and $\mathcal{C}_{\rm max}^{\rm TOV}$ to within 40% and 1.6%, respectively. Comparable results were obtained from smaller $q$'s.

The analogy between the definition of $K_{\rm eq}$ and the square of the speed of sound of NS matter, $c_{\rm s}^2=\partial P/\partial\epsilon|_{T=0,\delta_{\rm eq}}$, where $\epsilon$ is the density of internal energy, suggests that the measurement of the PC threshold at different $q$'s can also provide constraints on the value of $c_{\rm s}^2$ close to $n_{\rm max}^{\rm TOV}$. Indeed, the $\alpha$ and $\beta$ coefficients of Eq. (2) also correlate with $c_{\rm s}^2$ in a comparable way as with $K_{\rm max}$ and $\mathcal{C}_{\rm max}^{\rm TOV}$, as visible in the Supplemental Material [48]. Constraints on $c_{\rm s}$ can provide further insight into the physics governing the EOS of nuclear matter (see, e.g., Refs. [103,104]).

The larger detection horizon associated with massive BNS mergers suggests that, as in the case of GW190425 [105], PCs are a viable observational phenomenon associated with a significant fraction of BNSs that will become accessible in the next GW observing runs [106,107] and with third generation GW detectors [108–110]. While current GW detections allow the precise measurement of the chirp mass and, up to a certain extent, the total mass, the mass ratio is more uncertain. High enough signal-to-noise ratios and good sky localizations favoring followup EM observations will be key to provide better constraints on $q$. We estimate the possible impact of the uncertainties on $M_{\rm th}$ and on $q$ on the estimate of $K_{\rm max}$ by solving again Eq. (4), using the $\alpha'_{l,h}$ fitted coefficients (i.e., considering SFHo as our underlying EOS and removing it from our fitting sample). We randomly sample both $M_{\rm th}$ and $q$ within $M_{\rm th}\pm\Delta M_{\rm th}$ and $q\pm\Delta q$, where $\Delta M_{\rm th}$ and $\Delta q$ are the uncertainties in the determination of $M_{\rm th}(q)$. In the case of $q=0.85$ and $q=0.65$, to determine $K_{\rm max}$ with at least 30% accuracy at 90% confidence level, we estimate $\Delta M_{\rm th}\lesssim 0.025\ M_\odot$ and $\Delta q\lesssim 0.05$. For $q=0.85$ and $q=0.70$, the uncertainties should decrease to $\Delta M_{\rm th}\lesssim 0.01\ M_\odot$ and $\Delta q\lesssim 0.025$ to get a similar accuracy. The difference between the two cases proves that, due to the larger slope of $M_{\rm th}(q)$ at $q\ll 1$, the determination of $M_{\rm th}(q)$ for very asymmetric systems is more constraining. Such uncertainties are within reach of future observations and detectors [111]. More theoretical PC studies will be needed to reduce systematic uncertainties and include more detailed physics. Nevertheless, our results clearly indicate a new and unique way to access critical information on extreme density nuclear physics using observations of promptly collapsing BNS mergers.

A. Perego thanks Matteo Breschi for useful discussions. A. Perego, D. L., and S. B. acknowledge the INFN for the use of computing and storage resources through the Tullio cluster in Turin. The authors acknowledge the use of EOS tables from the CompOSE database [112]. D. L. thanks also C. Providencia for providing some EOS tables. A. Perego and D. L. acknowledge PRACE for awarding them access to Joliot-Curie at GENCI@CEA. A. Perego also acknowledges the use of computer resources under a CINECA-INFN agreement (allocation INF20_teongrav and INF21_teongrav). S. B. acknowledges funding from the EU H2020 under ERC Starting Grant No. BinGraSp-714626 and from the Deutsche Forschungsgemeinschaft (DFG) project MEMI No. BE 6301/2-1. D. R. acknowledges funding from the U.S. Department of Energy, Office of Science, Division of Nuclear Physics under Award No. DE-SC0021177 and from the National Science Foundation under Grants No. PHY-2011725, PHY-2020275, No. PHY-2116686, and No. AST-2108467. Numerical Relativity simulations were performed on Joliot-Curie at GENCI@CEA (PRACE-ra5202), SuperMUC-LRZ (Gauss project pn56zo), Marconi-CINECA (ISCRA-B project HP10BMHFQQ, INF20_teongrav, and INF21_teongrav allocation); Bridges, Comet, Stampede2 (NSF XSEDE allocation TG-PHY160025), NSF/NCSA Blue Waters (NSF AWD-1811236) supercomputers. This research used resources of the National Energy Research Scientific Computing Center, a DOE Office of Science User Facility supported by the Office of Science of the U.S. Department of Energy under Award No. DE-AC02-05CH11231.

*Corresponding author.
albino.perego@unitn.it

[1] J. M. Lattimer and M. Prakash, Phys. Rep. **621**, 127 (2016).
[2] M. Oertel, M. Hempel, T. Klähn, and S. Typel, Rev. Mod. Phys. **89**, 015007 (2017).
[3] R. Machleidt and D. R. Entem, Phys. Rep. **503**, 1 (2011).
[4] D. Chatterjee and I. Vidaña, Eur. Phys. J. A **52**, 29 (2016).
[5] D. Logoteta, Universe **7**, 408 (2021).
[6] I. Bombaci, D. Logoteta, I. Vidaña, and C. Providência, Eur. Phys. J. A **52**, 58 (2016).
[7] P. Braun-Munzinger and J. Wambach, Rev. Mod. Phys. **81**, 1031 (2009).
[8] S. Benic, D. Blaschke, D. E. Alvarez-Castillo, T. Fischer, and S. Typel, Astron. Astrophys. **577**, A40 (2015).
[9] U. Garg and G. Colò, Prog. Part. Nucl. Phys. **101**, 55 (2018).
[10] S. Shlomo, V. M. Kolomietz, and G. Colò, Eur. Phys. J. A **30**, 23 (2006).
[11] D. H. Youngblood, H. L. Clark, and Y. W. Lui, Phys. Rev. Lett. **82**, 691 (1999).
[12] J. R. Stone, N. J. Stone, and S. A. Moszkowski, Phys. Rev. C **89**, 044316 (2014).

[13] P. Avogadro and C. A. Bertulani, Phys. Rev. C **88**, 044319 (2013).
[14] P. Demorest, T. Pennucci, S. Ransom, M. Roberts, and J. Hessels, Nature (London) **467**, 1081 (2010).
[15] J. Antoniadis, P. C. Freire, N. Wex, T. M. Tauris, R. S. Lynch *et al.*, Science **340**, 6131 (2013).
[16] H. T. Cromartie *et al.* (NANOGrav Collaboration), Nat. Astron. **4**, 72 (2019).
[17] E. Fonseca *et al.*, Astrophys. J. Lett. **915**, L12 (2021).
[18] M. C. Miller *et al.*, Astrophys. J. Lett. **918**, L28 (2021).
[19] T. E. Riley *et al.*, Astrophys. J. Lett. **918**, L27 (2021).
[20] N.-B. Zhang and B.-A. Li, Astrophys. J. **921**, 111 (2021).
[21] B. P. Abbott *et al.* (LIGO Scientific, Virgo Collaborations), Phys. Rev. Lett. **121**, 161101 (2018).
[22] S. De, D. Finstad, J. M. Lattimer, D. A. Brown, E. Berger, and C. M. Biwer, Phys. Rev. Lett. **121**, 091102 (2018); **121**, 259902(E) (2018).
[23] D. Radice, A. Perego, F. Zappa, and S. Bernuzzi, Astrophys. J. **852**, L29 (2018).
[24] D. Radice and L. Dai, Eur. Phys. J. A **55**, 50 (2019).
[25] A. Bauswein, O. Just, H.-T. Janka, and N. Stergioulas, Astrophys. J. **850**, L34 (2017).
[26] B. Margalit and B. D. Metzger, Astrophys. J. **850**, L19 (2017).
[27] E. R. Most, L. R. Weih, L. Rezzolla, and J. Schaffner-Bielich, Phys. Rev. Lett. **120**, 261103 (2018).
[28] M. Breschi, A. Perego, S. Bernuzzi, W. Del Pozzo, V. Nedora, D. Radice, and D. Vescovi, Mon. Not. R. Astron. Soc. **505**, 1661 (2021).
[29] G. Raaijmakers, S. K. Greif, K. Hebeler, T. Hinderer, S. Nissanke, A. Schwenk, T. E. Riley, A. L. Watts, J. M. Lattimer, and W. C. G. Ho, Astrophys. J. Lett. **918**, L29 (2021).
[30] P. T. H. Pang, I. Tews, M. W. Coughlin, M. Bulla, C. Van Den Broeck, and T. Dietrich, Astrophys. J. **922**, 14 (2021).
[31] K. Hotokezaka, K. Kiuchi, K. Kyutoku, H. Okawa, Y. I. Sekiguchi, M. Shibata, and K. Taniguchi, Phys. Rev. D **87**, 024001 (2013).
[32] K. Hotokezaka, K. Kiuchi, K. Kyutoku, T. Muranushi, Y. I. Sekiguchi, M. Shibata, and K. Taniguchi, Phys. Rev. D **88**, 044026 (2013).
[33] A. Bauswein, S. Goriely, and H.-T. Janka, Astrophys. J. **773**, 78 (2013).
[34] M. Agathos, F. Zappa, S. Bernuzzi, A. Perego, M. Breschi, and D. Radice, Phys. Rev. D **101**, 044006 (2020).
[35] D. Radice, A. Perego, K. Hotokezaka, S. A. Fromm, S. Bernuzzi, and L. F. Roberts, Astrophys. J. **869**, 130 (2018).
[36] S. Bernuzzi *et al.*, Mon. Not. R. Astron. Soc. **497**, 1488 (2020).
[37] M. Shibata, K. Taniguchi, and K. Uryu, Phys. Rev. D **71**, 084021 (2005).
[38] K. Hotokezaka, K. Kyutoku, H. Okawa, M. Shibata, and K. Kiuchi, Phys. Rev. D **83**, 124008 (2011).
[39] A. Bauswein, T. W. Baumgarte, and H. T. Janka, Phys. Rev. Lett. **111**, 131101 (2013).
[40] S. Köppel, L. Bovard, and L. Rezzolla, Astrophys. J. **872**, L16 (2019).
[41] A. Bauswein and N. Stergioulas, J. Phys. G **46**, 113002 (2019).
[42] A. Bauswein, S. Blacker, V. Vijayan, N. Stergioulas, K. Chatziioannou, J. A. Clark, Niels-Uwe F. Bastian, D. B. Blaschke, M. Cierniak, and T. Fischer, Phys. Rev. Lett. **125**, 141103 (2020).
[43] R. Kashyap, A. Das, D. Radice, S. Padamata, A. Prakash, D. Logoteta, A. Perego, D. A. Godzieba, S. Bernuzzi, I. Bombaci, F. J. Fattoyev, B. T. Reed, and A. S. Schneider, Phys. Rev. D **105**, 103022 (2022).
[44] A. Bauswein, S. Blacker, G. Lioutas, T. Soultanis, V. Vijayan, and N. Stergioulas, Phys. Rev. D **103**, 123004 (2021).
[45] S. D. Tootle, L. J. Papenfort, E. R. Most, and L. Rezzolla, Astrophys. J. Lett. **922**, L19 (2021).
[46] M. Kölsch, T. Dietrich, M. Ujevic, and B. Bruegmann, arXiv:2112.11851.
[47] A. Bauswein, H. T. Janka, K. Hebeler, and A. Schwenk, Phys. Rev. D **86**, 063001 (2012).
[48] See Supplemental Material at http://link.aps.org/supplemental/10.1103/PhysRevLett.129.032701 for a detailed description of the simulation setup, simulation results, extended equation of state sample, and alternative fits.
[49] D. Radice and L. Rezzolla, Astron. Astrophys. **547**, A26 (2012).
[50] D. Radice, L. Rezzolla, and F. Galeazzi, Mon. Not. R. Astron. Soc. **437**, L46 (2014).
[51] D. Radice, L. Rezzolla, and F. Galeazzi, Classical Quantum Gravity **31**, 075012 (2014).
[52] F. Loffler *et al.*, Classical Quantum Gravity **29**, 115001 (2012).
[53] S. Bernuzzi and D. Hilditch, Phys. Rev. D **81**, 084003 (2010).
[54] D. Hilditch, S. Bernuzzi, M. Thierfelder, Z. Cao, W. Tichy, and B. Brugmann, Phys. Rev. D **88**, 084057 (2013).
[55] D. Pollney, C. Reisswig, E. Schnetter, N. Dorband, and P. Diener, Phys. Rev. D **83**, 044045 (2011).
[56] C. Reisswig, C. D. Ott, E. Abdikamalov, R. Haas, P. Mösta, and E. Schnetter, Phys. Rev. Lett. **111**, 151101 (2013).
[57] E. Schnetter, S. H. Hawley, and I. Hawke, Classical Quantum Gravity **21**, 1465 (2004).
[58] M. J. Berger and J. Oliger, J. Comput. Phys. **53**, 484 (1984).
[59] M. J. Berger and P. Colella, J. Comput. Phys. **82**, 64 (1989).
[60] F. Galeazzi, W. Kastaun, L. Rezzolla, and J. A. Font, Phys. Rev. D **88**, 064009 (2013).
[61] D. Radice, F. Galeazzi, J. Lippuner, L. F. Roberts, C. D. Ott, and L. Rezzolla, Mon. Not. R. Astron. Soc. **460**, 3255 (2016).
[62] E. Gourgoulhon, P. Grandclement, K. Taniguchi, J.-A. Marck, and S. Bonazzola, Phys. Rev. D **63**, 064029 (2001).
[63] M. Alford, M. Braby, M. W. Paris, and S. Reddy, Astrophys. J. **629**, 969 (2005).
[64] F. J. Fattoyev, J. Piekarewicz, and C. J. Horowitz, Phys. Rev. Lett. **120**, 172702 (2018).
[65] J. M. Pearson, S. Goriely, and N. Chamel, Phys. Rev. C **83**, 065810 (2011).
[66] J. M. Pearson, N. Chamel, S. Goriely, and C. Ducoin, Phys. Rev. C **85**, 065803 (2012).

[67] V. Dexheimer and S. Schramm, Astrophys. J. **683**, 943 (2008).
[68] V. Dexheimer, R. Negreiros, and S. Schramm, Phys. Rev. C **92**, 012801(R) (2015).
[69] N.-U. F. Bastian, Phys. Rev. D **103**, 023001 (2021).
[70] F. Douchin and P. Haensel, Astron. Astrophys. **380**, 151 (2001).
[71] M. Oertel, C. Providência, F. Gulminelli, and A. R. Raduta, J. Phys. G **42**, 075202 (2015).
[72] M. Fortin, S. S. Avancini, C. Providência, and I. Vidaña, Phys. Rev. C **95**, 065803 (2017).
[73] N. K. Glendenning and S. A. Moszkowski, Phys. Rev. Lett. **67**, 2414 (1991).
[74] B. D. Lackey, M. Nayyar, and B. J. Owen, Phys. Rev. D **73**, 024021 (2006).
[75] J. S. Read, C. Markakis, M. Shibata, K. Uryu, J. D. E. Creighton, and J. L. Friedman, Phys. Rev. D **79**, 124033 (2009).
[76] N. Jokela, M. Järvinen, G. Nijs, and J. Remes, Phys. Rev. D **103**, 086004 (2021).
[77] X. Roca-Maza, X. Vinas, M. Centelles, P. Ring, and P. Schuck, Phys. Rev. C **84**, 054309 (2011); **93**, 069905(E) (2016).
[78] H. Müther, M. Prakash, and T. L. Ainsworth, Phys. Lett. B **199**, 469 (1987).
[79] H. Müller and B. D. Serot, Nucl. Phys. **A606**, 508 (1996).
[80] G. Shen, C. J. Horowitz, and S. Teige, Phys. Rev. C **83**, 035802 (2011).
[81] K. Otto, M. Oertel, and B.-J. Schaefer, Phys. Rev. D **101**, 103021 (2020).
[82] K. Otto, M. Oertel, and B.-J. Schaefer, Eur. Phys. J. Special Topics **229**, 3629 (2020).
[83] G. Baym, T. Hatsuda, T. Kojo, P. D. Powell, Y. Song, and T. Takatsuka, Rep. Prog. Phys. **81**, 056902 (2018).
[84] G. Baym, S. Furusawa, T. Hatsuda, T. Kojo, and H. Togashi, Astrophys. J. **885**, 42 (2019).
[85] F. Gulminelli and A. R. Raduta, Phys. Rev. C **92**, 055803 (2015).
[86] E. Chabanat, P. Bonche, P. Haensel, J. Meyer, and R. Schaeffer, Nucl. Phys. **A635**, 231 (1998); **A643**, 441(E) (1998).
[87] A. S. Schneider, L. F. Roberts, and C. D. Ott, Phys. Rev. C **96**, 065802 (2017).
[88] H. Shen, H. Toki, K. Oyamatsu, and K. Sumiyoshi, Nucl. Phys. **A637**, 435 (1998).
[89] M. Hempel, T. Fischer, J. Schaffner-Bielich, and M. Liebendorfer, Astrophys. J. **748**, 70 (2012).
[90] D. Logoteta, I. Bombaci, and A. Perego, Eur. Phys. J. A **58**, 55 (2022).
[91] Y. Sugahara and H. Toki, Nucl. Phys. **A579**, 557 (1994).
[92] I. Bombaci and D. Logoteta, Astron. Astrophys. **609**, A128 (2018).
[93] D. Logoteta, A. Perego, and I. Bombaci, Astron. Astrophys. **646**, A55 (2021).
[94] A. W. Steiner, M. Hempel, and T. Fischer, Astrophys. J. **774**, 17 (2013).
[95] S. Typel, G. Ropke, T. Klahn, D. Blaschke, and H. H. Wolter, Phys. Rev. C **81**, 015803 (2010).
[96] M. Hempel and J. Schaffner-Bielich, Nucl. Phys. **A837**, 210 (2010).
[97] J. M. Lattimer and F. D. Swesty, Nucl. Phys. **A535**, 331 (1991).
[98] S. Banik, M. Hempel, and D. Bandyopadhyay, Astrophys. J. Suppl. Ser. **214**, 22 (2014).
[99] K. Kiuchi, K. Kawaguchi, K. Kyutoku, Y. Sekiguchi, and M. Shibata, Phys. Rev. D **101**, 084006 (2020).
[100] T. Dietrich, N. Moldenhauer, N. K. Johnson-McDaniel, S. Bernuzzi, C. M. Markakis, B. Brügmann, and W. Tichy, Phys. Rev. D **92**, 124007 (2015).
[101] T. Dietrich, M. Ujevic, W. Tichy, S. Bernuzzi, and B. Brügmann, Phys. Rev. D **95**, 024029 (2017).
[102] H. Togashi, K. Nakazato, Y. Takehara, S. Yamamuro, H. Suzuki, and M. Takano, Nucl. Phys. **A961**, 78 (2017).
[103] I. Tews, J. Carlson, S. Gandolfi, and S. Reddy, Astrophys. J. **860**, 149 (2018).
[104] C. D. Capano, I. Tews, S. M. Brown, B. Margalit, S. De, S. Kumar, D. A. Brown, B. Krishnan, and S. Reddy, Nat. Astron. **4**, 625 (2020).
[105] B. Abbott *et al.* (LIGO Scientific, Virgo Collaborations), Astrophys. J. Lett. **892**, L3 (2020).
[106] B. P. Abbott *et al.* (Virgo, KAGRA, LIGO Scientific Collaborations), Living Rev. Relativity **21**, 3 (2018); **19**, 1 (2016).
[107] B. P. Abbott *et al.* (KAGRA, LIGO Scientific, Virgo Collaborations), Living Rev. Relativity **21**, 3 (2018).
[108] M. Punturo, M. Abernathy, F. Acernese, B. Allen, N. Andersson *et al.*, Classical Quantum Gravity **27**, 194002 (2010).
[109] M. Maggiore *et al.*, J. Cosmol. Astropart. Phys. 03 (2020) 050.
[110] D. Reitze *et al.*, Bull. Am. Astron. Soc. **51**, 035 (2019).
[111] S. Borhanian and B. S. Sathyaprakash, arXiv:2202.11048.
[112] https://compose.obspm.fr/.